ORIGINAL ARTICLE

Atypical rheology and spinning behavior of poly(vinyl alcohol) in a nonaqueous solvent

Deepika Gupta[1] · Manjeet Jassal[1] · Ashwini K. Agrawal[1]

Abstract

Electrospinning poly(vinyl alcohol), which is an important water-soluble biopolymer, using an organic solvent, such as dimethyl sulfoxide (DMSO), is particularly important for applications such as the controlled release of drugs with poor solubility in water. Since the nature of the solvent can greatly influence the morphology of the nanofibers and hence their bio-applicability, the rheology and electrospinning behavior of PVA in DMSO were investigated and compared with those in water. The viscosity, storage modulus and elasticity were found to be higher for PVA solutions in DMSO than in water for the same concentration of PVA. However, the fiber diameter obtained from the PVA-DMSO system was significantly lower. Although a linear correlation between the fiber diameter and elasticity could be established for the two solvents, their slopes were different. In a further investigation, a single linear equation could be determined for the two systems to give the relationship between the diameter and the number of entanglements per chain, suggesting that elasticity arising from chain entanglements was the key factor governing the fiber diameter.

Introduction

PVA nanofibers have been extensively used for biomedical applications, such as drug delivery [1] and protein release systems [2], nanobiocomposites for wound dressing [3] and composite nanofibers for tissue engineering [4]. PVA is a preferred polymer because of its biodegradability, biocompatibility and easy processability with other polymers and materials in aqueous solvents [5, 6]. The rheological properties and electrospinning behavior of PVA in water are well documented [7–10]. However, the electrospinning of PVA in an organic solvent is particularly important for applications such as the controlled delivery of drugs that have low aqueous solubility but good solubility in organic solvents [11]. Consequently, Mano et al. used encapsulated natural deep eutectic solvent as an alternative solvent for electrospinning PVA [12].

DMSO is another solvent for PVA, and interestingly, it has been reported to be a better solvent (for PVA) than water [13–16]. This is because the intrinsic viscosity [η] of PVA in DMSO is 3.25 dL/g, which is higher than that in water, 0.93 dL/g [14–17]. Young et al. [15] have shown using Flory-Huggins theory that the interaction parameter, χ, of water/PVA is 0.509 and that of DMSO/PVA is 0.328, implying better interactions of PVA with DMSO [17]. The Hildebrand solubility parameters of DMSO and PVA are ~12.9 and 12.6 δ ($cal^{1/2}cm^{-3/2}$), respectively, which are nearly the same, while that of water is distinctly different at 23.5 δ ($cal^{1/2}cm^{-3/2}$).

DMSO has numerous applications in areas such as analytical chemistry, biology, and medicine [18]. DMSO has very low toxicity, making it suitable as a pharmaceutical agent in addition to being an effective solvent. Additionally, the presence of DMSO has been shown to enhance the dispersibility of various nanomaterials in PVA, facilitating the preparation of composite fibers [19]. The solution properties, such as the evaporation rate, dielectric constant, conductivity, and surface tension, are influenced by the nature of the solvent and affect the nanofiber morphology [20–23]. Additionally, the nature of the solvent also affects the rheological properties of a polymer solution, such as its viscosity and elasticity [24–26]. Kong et al. demonstrated the electrospinning of starch using DMSO as a solvent

✉ Manjeet Jassal
manjeetjassal@gmail.com

1 SMITA Research Lab, Department of Textile Technology, Indian Institute of Technology-Delhi, Hauz Khas, New Delhi 110016, India

because it dissolved the starch completely, thereby providing sufficient entanglements for fiber electrospinning [27]. PVA has been reported to display unusual rheological behavior in mixtures of DMSO-water [28]. The effects of the DMSO-water (binary solvent) composition on the rheology and electrospinning behavior have also been enumerated in our previous study [29]. It has been shown that as the DMSO-water molar ratio changes, the heterogeneity of the solution is increased, which in turn affects the rheology as well as fiber morphology at the same concentration of PVA.

Our previous studies [30–32] have also established that the solution properties are the primary factors affecting the electrospinning process, and among them, the elasticity of a polymeric solution plays a major role in controlling the fiber diameter [33]. However, the influence of the nature of the solvent on rheological properties and its role in controlling nanofiber diameter has not been studied.

In this study, we investigated the electrospinning behavior of PVA in two different solvents, i.e., DMSO and water, and correlated the morphology, i.e., the diameter, of the nanofibers obtained from these solutions with their rheological properties.

Experimental section

High-molecular-weight PVA ($M_w \sim 125,000$) was purchased from Central Drug House, New Delhi, India. Deionized water (DI) and dimethyl sulfoxide (Merck, India) were used as solvents.

Preparation of solutions

PVA solutions in DMSO at concentrations of 8, 10, 12, 14, 16, 18 and 20 wt% were prepared by dissolving the required amount of PVA in DMSO at 90 °C with constant stirring until clear solutions were obtained (Table 1). Similarly, aqueous solutions of PVA at concentrations of 4, 6, 8, 10,

12, 14 and 16 wt% were prepared in DI water at 80 °C (Table 2). The solutions were equilibrated at 35 °C prior to their electrospinning and rheological characterization.

Rheological characterization of PVA solutions

The shear rheology of the PVA solutions was characterized using a rotational rheometer (MCR 302, Anton Paar GmBh, Germany) with a 50-mm diameter and 1° cone-plate geometry at 35 °C. The strain amplitude (γ°) as obtained from the amplitude sweep was kept at 10%. The steady-state measurements were conducted at shear rates from 0.1 to $1000 \, s^{-1}$. Frequency sweeps were conducted from 0.1 to 100 rad/s. Multiple readings for two different sets of solutions were measured, and reproducible values have been reported.

Electrospinning of PVA solutions

A bipolar high-voltage power supply (D-ES40PN-10W, Gamma High Voltage Research, Ormond Beach, FL, USA) was used for electrospinning. The polymer droplet was charged by connecting the spinning needle to a positive voltage and the collector to a negative voltage. The polymer solutions were extruded using a syringe pump (model KDS-100-CE, KD Scientific, Holliston, MA, USA), a 2-ml syringe and a blunted 18-G needle. The fibers were deposited on a circular aluminum plate used as the collector. Nanofiber samples were collected at flow rates of 0.5 ml/h and a spinning distance of 20 cm. The electrospinning was carried out in a chamber maintained at 35 °C and a relative humidity of 40% to ensure efficient evaporation of the solvents. The obtained electrospun fibers were vacuum dried overnight before characterization.

Surface morphology of the electrospun nanofibers

The surface morphology of the fibers was evaluated using scanning electron microscopy (Quanta 200 F, FEI,

Table 1 Rheological parameters and fiber diameter for PVA-DMSO

Sample code for PVA-DMSO solutions	Viscosity (Pa.s)	Specific viscosity	Storage modulus (Pa)	Compliance (1/Pa)	Relaxation time (ms)	Diameter (nm)
6 PVA-D	0.38	196.89	5.67	0.000707	–	–
8 PVA-D	0.69	362.15	6.7	0.00141	0.94	45 + droplets
10 PVA-D	2.11	1109.52	28.28	0.000942	1.93	63 ± 35
12 PVA-D	4.13	2172.68	89.68	0.000623	2.50	88 ± 24
14 PVA-D	9.08	4777.94	235.36	0.000451	3.72	145 ± 31
16 PVA-D	18.98	9991.10	516.01	0.000272	4.81	203 ± 28
18 PVA-D	39.4	20735.84	1186.65	0.000189	6.92	272 ± 38
20 PVA-D	70.5	37104.26	2238.13	0.000128	8.71	370 ± 41

Table 2 Rheological parameters and fiber diameter for PVA-water

Sample code for PVA-water solutions	Viscosity (Pa.s)	Specific viscosity	Storage modulus (Pa)	Compliance (1/Pa)	Relaxation time (ms)	Diameter (nm)
2 PVA-W	0.0039	20	0.22	–	–	–
4 PVA-W	0.0188	89.1	0.21	–	–	80 ± 14
6 PVA-W	0.0742	275	0.859	0.0499	1.09	120 ± 15
8 PVA-W	0.2511	354.3	3.5	0.013	1.69	155 ± 24
10 PVA-W	0.7199	766	12.5	0.0026	1.84	238 ± 32
12 PVA-W	1.825	1936	38.76	0.0013	2.28	333 ± 27
14 PVA-W	3.91	4070	84.17	0.0009	3.42	445 ± 49
16 PVA-W	8.83	9009	204.76	0.0006	4.89	638 ± 56

Netherlands). The fiber diameters were determined using ImageJ software. For each sample, the average diameter of two hundred fibers along with the standard deviation is reported. Statistical analysis was performed using Student's t-test using equal variance for unpaired samples and a two-tailed test.

Mechanical testing

Nanofibrous webs of PVA in DMSO and water were tested for their mechanical strength using an Instron microtensile tester (Model 5848, Singapore) at a crosshead speed of 5 mm/min and a load cell capacity of 10 N. Samples (length of 2.5 cm and width of 1.0 cm) were prepared using 14 wt% PVA in water and 22 wt% PVA in DMSO, as the diameters of the fibers obtained from these solutions were found to be similar. Since the concentrations of PVA in the two solvents were different, the same amount of polymer was deposited by adjusting the flow rate and time of deposition to obtain comparable samples. An average value of five specimens has been reported.

Thermal analysis

Thermal analysis of the nanofiber webs obtained from the spinning of PVA in the two solvents i.e., water and DMSO, were performed using differential scanning calorimetry (DSC Q200, TA Instruments, New Castle, DE, USA).

Results and discussion

Rheological characterization

Figure 1 shows the viscosity curve with increasing shear rates for PVA solutions in DMSO and in water. As expected, the viscosities of both the PVA-DMSO and PVA-water solutions increased with increasing concentration. PVA-DMSO solutions upto 14 wt% show Newtonian
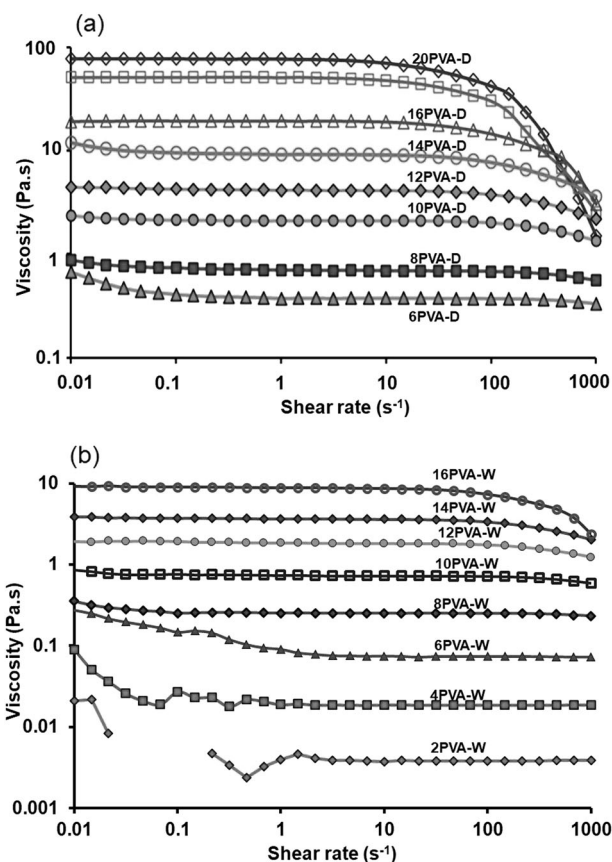

Fig. 1 Viscosity vs. shear rate plots for PVA solutions at 35 °C in (**a**) DMSO and (**b**) water. where η_s is the solvent viscosity

behavior for shear rates ranging from 0.01 to $100\,\mathrm{s}^{-1}$. At higher concentrations of 16, 18 and 20 wt%, shear thinning behavior was observed beyond a shear rate of $10\,\mathrm{s}^{-1}$. In the case of PVA-water solutions, a shear thinning effect was observed for concentrations beyond 12 wt% beyond a shear rate of $50\,\mathrm{s}^{-1}$. Comparing the two polymer-solvent systems, it was observed that for the same concentration of PVA, the viscosity was higher in DMSO than in water. For example, for a 16 wt% PVA solution, the viscosity in water at a shear rate of $10\,\mathrm{s}^{-1}$ was 8.63 Pa.s, while in DMSO, it was

significantly higher at 18.97 Pa.s. The results indicate that PVA has a more extended conformation in DMSO because there are more intermolecular chain interactions. In the case of PVA-water, the polymer chains are in a coiled conformation with strong intramolecular interactions. Compared to collapsed or coiled chains, extended chains offer more resistance to flow as their effective volume is greater than the critical volume.

Concentration regions of PVA in DMSO and water were determined using steady shear measurements. The zero shear viscosity (η_0) was determined for all concentrations from the viscosity vs. shear rate curves by extrapolating to a zero shear rate. Specific viscosities were calculated using Eq. 1.

$$\eta_{sp} = (\eta_0 - \eta_s)/\eta_s, \tag{1}$$

where η_s is the solvent viscosity.

The zero shear viscosity, which was determined from the viscosity-shear rate curves, was found to increase from 0.021 to 9.01 Pa.s for PVA-water solutions as the concentration was increased from 2 to 16 wt%. It may be noted that the 2PVA-W sample had a very low viscosity; therefore, the curve was scattered with missing points at the low shear rates. This was due to insufficient responses from the sample that were below the instrument threshold. For PVA-DMSO solutions, the zero shear viscosity increased from 0.408 to 77.0 Pa.s as the concentration of PVA was increased from 6 to 20 wt%. Figure 2 shows the plots of the specific viscosity (η_{sp}) as a function of the PVA concentration for both the PVA-water and PVA-DMSO solutions.

The figure shows three distinct concentration regions for both systems. For the PVA-DMSO solutions (Fig. 2a), the semidilute unentangled region, where $\boldsymbol{\eta_{sp} \sim c^{1.48}}$, and the semidilute entangled region, where $\eta_{sp} \sim c^{4.59}$, were similar to the previously reported values of $\eta_{sp} \sim c^{1.26}$ and $\eta_{sp} \sim c^{4.8}$ respectively, for linear polymer solutions in good solvents [34]. Furthermore, the specific viscosity in the concentrated region, where $\eta_{sp} \sim c^{5.99}$, shows a stronger dependence on the concentration compared to that reported in the literature, where $\eta_{sp} \sim c^{3.8}$. The change in the slope from the semidilute unentangled to the semidilute entangled region marks the entanglement concentration (C_e), which is ~10 wt% for the PVA-DMSO system. The start of the concentrated region (C^{**}) was indicated by a change in slope at ~14 wt%. On the other hand, for the PVA-water solutions (Fig. 2b), the semidilute unentangled, semidilute entangled and concentrated regions show a scaling relationship of $\eta_{sp} \sim c^{2.1}$, $\eta_{sp} \sim c^{3.45}$ and $\eta_{sp} \sim c^{5.33}$, respectively. The entanglement concentration (C_e) and the start of the concentrated region (C^{**}) for PVA-water were at ~7 and ~11 wt%, respectively, which were significantly lower than those of PVA-DMSO solutions.
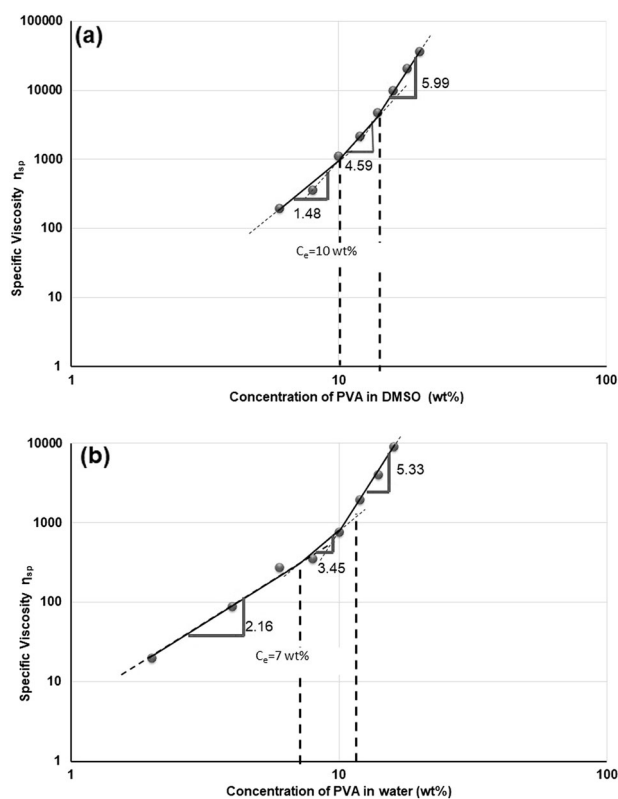

Fig. 2 Specific viscosity vs. concentration plots for PVA solutions in (**a**) DMSO and (**b**) water

Figure 3 shows the frequency sweep plots for the storage (G′) and loss (G″) modulus with respect to the angular frequency for both the PVA-DMSO and PVA-water solutions. The values of both G′ and G″ increase with increasing PVA concentration for both solvents. However, at the same concentrations of PVA, the values of G′ and G″ were found to be higher in DMSO than in water. Ideally, for homogeneous solutions, the slope for the storage modulus should be 2. However, the slopes of G′ in the angular frequency range of 10 to 100 rad/s varied from 1.347 to 1.25 for different concentrations of PVA in DMSO.

Similarly, for the PVA-water system, the slope varied from 1.31 to 1.27 with increasing concentration. The decrease in the slope with increasing PVA concentration can be attributed to an increase in the inter- and intramolecular hydrogen bonding in PVA.

Figure 4 shows the modified Cole-Cole plots for PVA in DMSO and water solutions in the range of 10 to 100 rad/s. The Cole-Cole plot represents the ratio of G′ to G″. Ideally, for homogenous solutions, the slope of the Cole-Cole plot is 2. The slope of the PVA-DMSO solutions was close to 2 (~1.81) for all the concentrations, while for the PVA-water solutions, the slopes were lower and varied in the range of 1.68 to 1.79 for the different concentrations. This suggests that the solutions of PVA-DMSO are relatively more
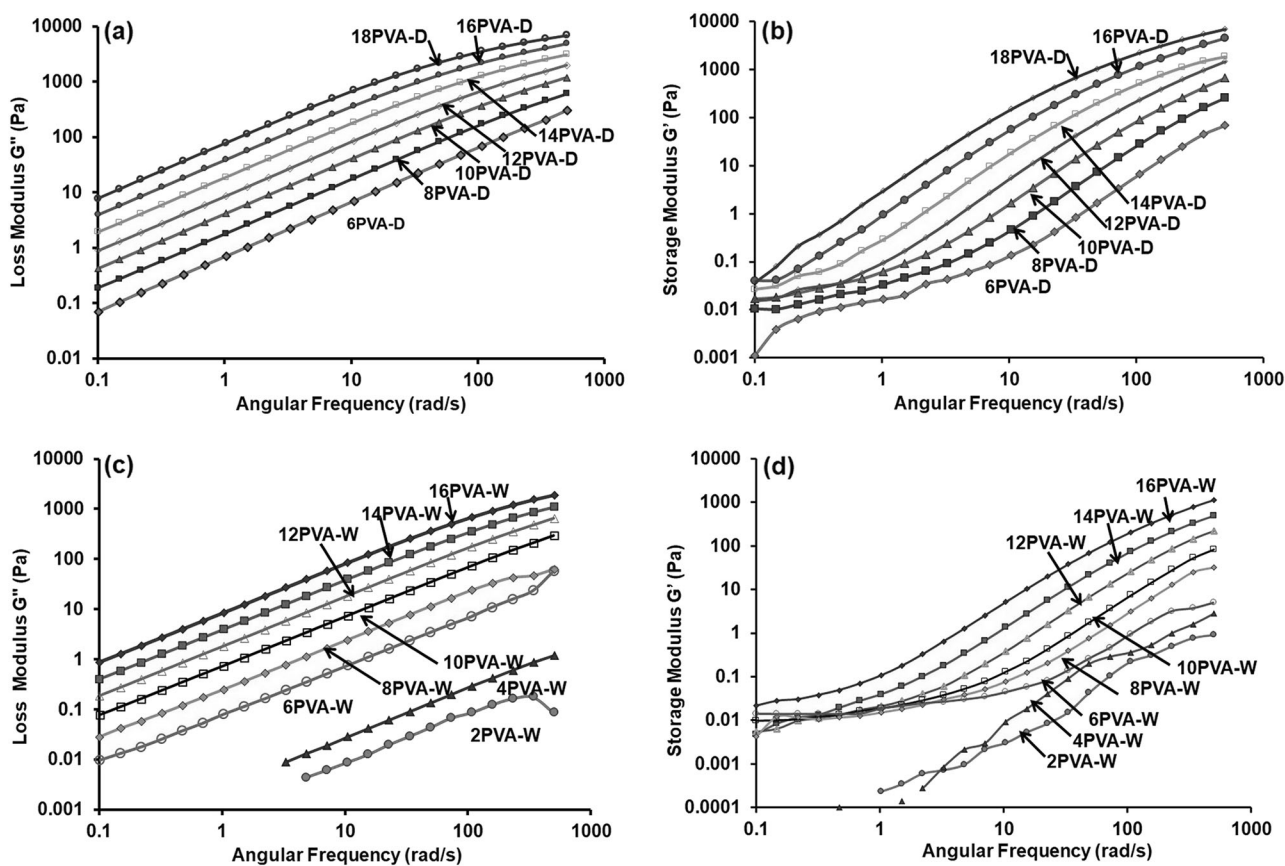
Fig. 3 Plots of loss and storage modulus for PVA solutions in DMSO (**a**, **b**) and water (**c**, **d**)

homogenous than the PVA-water solutions due to the better solubility of PVA in DMSO. The slope being slightly lower than 2 can be attributed to the inherent ability of PVA to form strong inter- and intramolecular hydrogen bonds in solutions.

PVA is known to form strong gels in both DMSO and water when quenched at lower temperatures, and the gelling tendency increases with increasing PVA concentration. To understand the type of inhomogeneity in PVA solutions, the values of tan (δ) vs. angular frequency for the PVA-DMSO and PVA-water solutions were plotted. These plots are shown in Fig. 5. Tan (δ) values >1 signify the solution phase, while value ≤1 signify solid-like behavior. From the figure, it can be clearly seen that PVA-DMSO solutions at concentrations of 6–14 wt% show solution-like behavior across the entire frequency range. However, PVA-DMSO solutions of 16 and 18 wt% tend to show solid-like behavior at very high frequencies, as their tan (δ) values approaches 1. This can occur only when there is a higher degree of chain-chain interactions. Since the chains are in extended conformations in the DMSO system with bulky DMSO molecules strongly associated with the main chain, it is proposed that such chains may become aligned in the

direction of the shear and thus come closer to show higher levels of chain overlap and bulky group interactions. In the case of PVA-water, none of the solutions regardless of concentration showed any change in the phase behavior, as their tan (δ) values are higher than 1.

The results indicate that all the solutions are in the liquid phase over most of the studied frequency range. This implied that the inhomogeneity observed in the Cole-Cole plot (i.e., slope value less than 2) is not due to liquid-solid-type phase separation but is likely due to liquid-liquid demixing of the PVA solutions [29]. Furthermore, the lower slope of the PVA-water solution in the Cole-Cole plot suggests that the liquid-liquid phase separation tendency is slightly higher in water than in DMSO.

Electrospinning of the PVA solutions

PVA-DMSO: Solutions of PVA-DMSO (6 to 20 wt%) were electrospun. The obtained fibers were viewed by FESEM, and the images are shown in Fig. 6. The electrospinning of solutions up to 10 wt% PVA content (images of 6 and 8 wt% are not shown) resulted in the formation of beads and droplets along with fine fibers. The 10 wt% PVA-DMSO
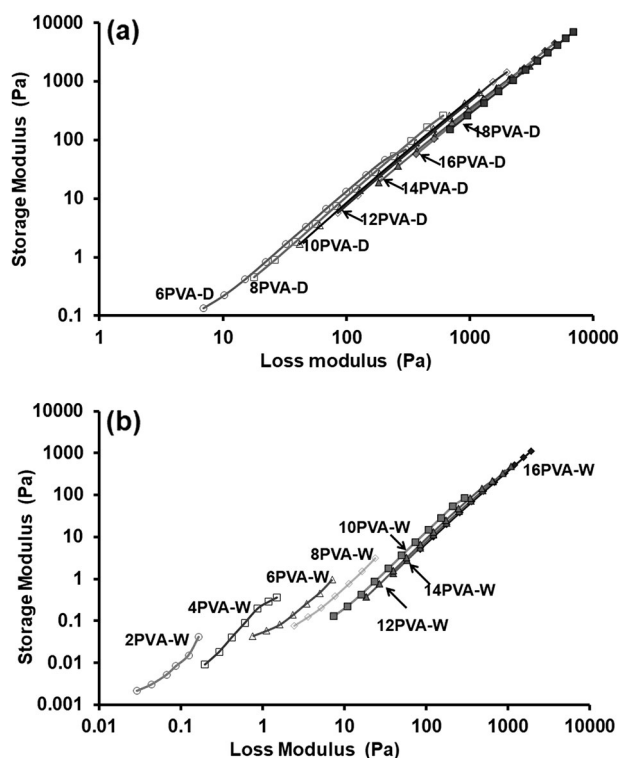
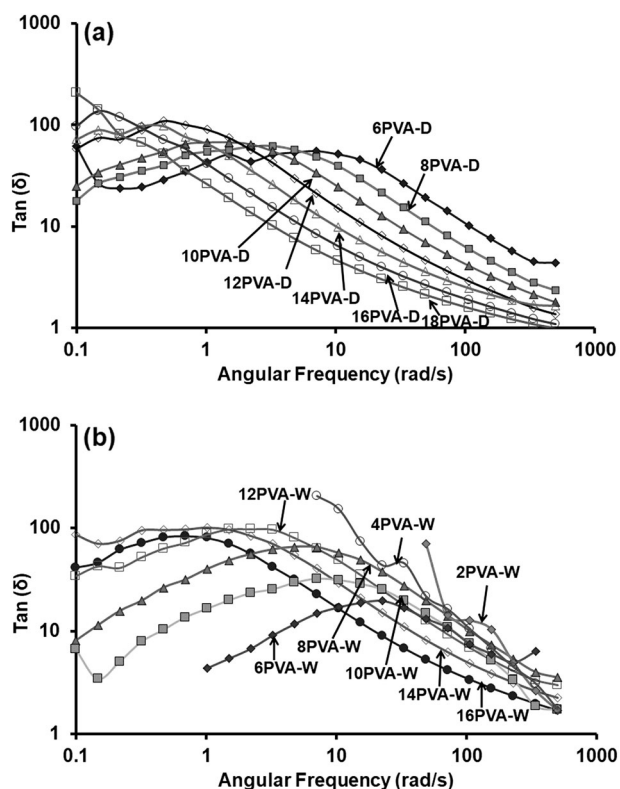**Fig. 4** Modified Cole-Cole plots for PVA solutions in (**a**) DMSO and (**b**) water

Fig. 5 Plots of tan (δ) vs. angular frequency for PVA solutions in (**a**) DMSO and (**b**) water

solution was electrospun at 18 kV. The 12 wt% PVA-DMSO solution spun at 16.5 kV resulted in fibers with a few elongated beads, while solutions of 14, 16, 18, and 20 wt% spun at 15, 14.5, 13 and 12.5 kV gave defect-free fibers. The fiber diameters increased from 88 ± 24 nm to 370 ± 41 nm as the concentration of PVA was increased from 12 to 20 wt%. Table 1 summarizes the diameters of all the nanofibers. The observations may be attributed to the entanglement concentration (C_e), which is 10 wt% in the case of PVA-DMSO. This is the minimum concentration necessary to obtain good fibers. However, defect-free uniform fibers could be realized only when the concentration was in the concentrated region, i.e., above C** of ~14 wt%.

PVA-water: Solutions of PVA-water (6–16%) were electrospun, and the obtained fibers were observed by FESEM (Fig. 7). The PVA-water solutions with concentrationslower than 6 wt% formed nonuniform fibers and beads (images of 2 and 4 wt% not shown). Although the entanglement concentration (C_e) for PVA-water was found to be 7 wt%, fine fibers with only a few elongated beads could be obtained at a slightly lower concentration of 6 wt% (spun at 18 kV). At higher PVA concentrations (i.e., above 6 wt%), smooth and uniform fibers were obtained. PVA-water solutions of 8, 10, 12, 14 and 16 wt% were electrospun at 16, 15, 13, 12.5 and 11 kV, respectively. The diameters of the fibers increased with increasing polymer concentration and ranged from 120 ± 15 (for 6 wt%) to 638 ± 56 nm (for 16 wt%). The fiber diameters obtained from various concentrations of PVA-water are summarized in Table 2.

A very interesting observation was made when the results of the two solvent systems were compared. For the same concentrations of PVA, the obtained fiber diameters were significantly higher when water was used as the solvent (compared to DMSO) even though the viscosity and storage modulus were much lower in water.

Correlation of the solution properties of PVA-DMSO and PVA-water with the fiber diameter

Solution properties play a vital role in determining the fiber diameters. The diameters of the nanofibers obtained from both PVA-DMSO and PVA-water solutions were plotted against the dynamic viscosity (η) of the solutions (Fig. 8). From the figure, it may be observed that both the viscosity and diameter increase with increasing PVA concentration. However, the slope of the plot of the diameter and the viscosity decreases with increasing viscosity. This indicates that the dependence of diameter on the viscosity decreases with an increase in the concentration of the PVA solutions. This effect is more pronounced in the case of DMSO, where a saturating effect on the diameter of the nanofibers can be seen. According to Graessley [35] and Colby et al. [36],

Fig. 6 SEM images of nanofibers obtained from PVA-DMSO solutions of different concentrations
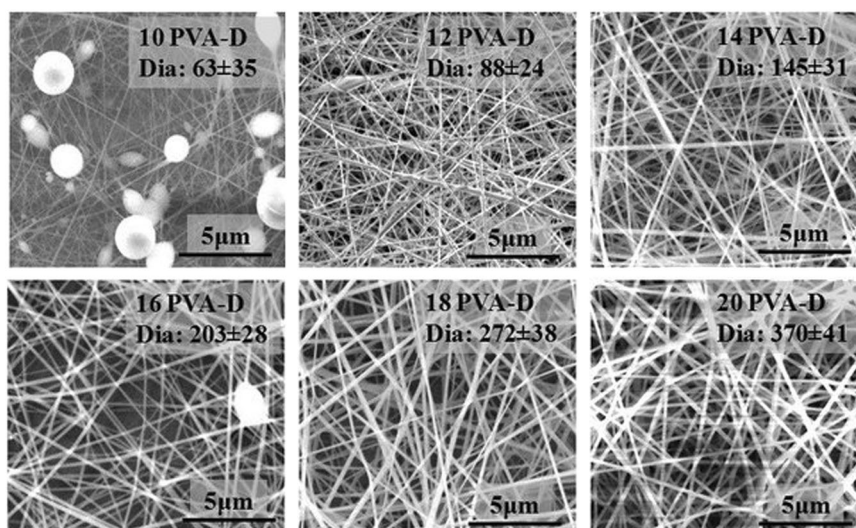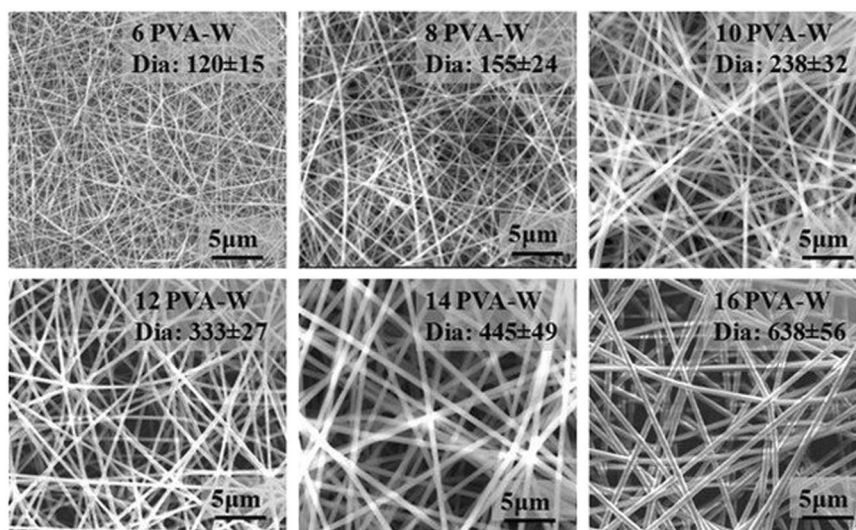

Fig. 7 SEM images of nanofibers obtained from PVA-water solutions of different concentrations

when the concentration is increased into the concentrated region, the flow behavior is dominated by chain entanglements, represented by $\Phi_p M_w$ [37], rather than $c[\eta]$, which is true for dilute solutions. This implies that the electrospun fiber diameters cannot be well correlated with the viscosity values obtained at high concentrations. This observation is supported by the findings of our previous work [33] on Boger fluids (PVA-based compositions having similar viscosities), where fiber diameter was found to be directly dependent on the relaxation time of the solutions.

The elasticity of a polymeric solution is expressed in terms of its relaxation time (λ) and can be calculated using Eq. 2 based on the Maxwell model [38].

$$\lambda = \left[G'/\omega^2 \right]/\eta, \tag{2}$$

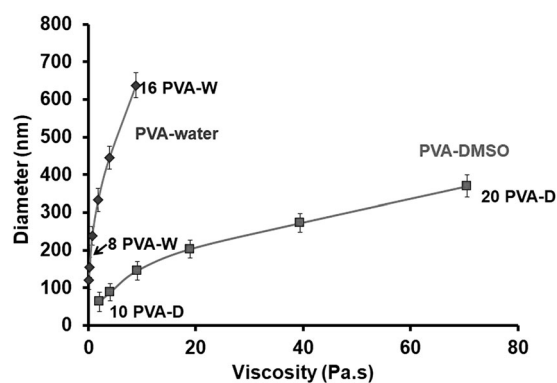where η is the apparent viscosity and ω is the angular frequency.

Fig. 8 Plots of fiber diameter vs. viscosity for PVA-DMSO and PVA-water systems

However, when DMSO is used as the solvent, the PVA chains take on an extended conformation as explained earlier and become surrounded by DMSO molecules, which

form hydrogen bonds. Because of this extended conformation, the extent of the interchain interactions increases, which leads to the formation of pseudostructures, as explained by Gao et al. [39] and Cho et al. [40]. Extended chain conformations result in a higher viscosity, while pseudostructures result in higher relaxation times. For such systems involving pseudostructures, the relaxation time can be calculated using Eq. 3:

$$J' = \lambda / |\eta^*|, \tag{3}$$

where J' is the compliance and η^* is the complex viscosity of the solution measured at $\omega \sim 100$ rad/s. At this frequency, all the polymer solutions showed stable shear viscosities, and therefore, the calculated relaxation time values can be used to evaluate the relative elasticities of the polymer solutions.

The diameters of the nanofibers obtained from both PVA-DMSO and PVA-water were plotted against the relaxation time, which was calculated using Eq. 3 and are shown in Fig. 9. It can be clearly seen that the fiber diameters for both polymer-solvent systems are linearly related
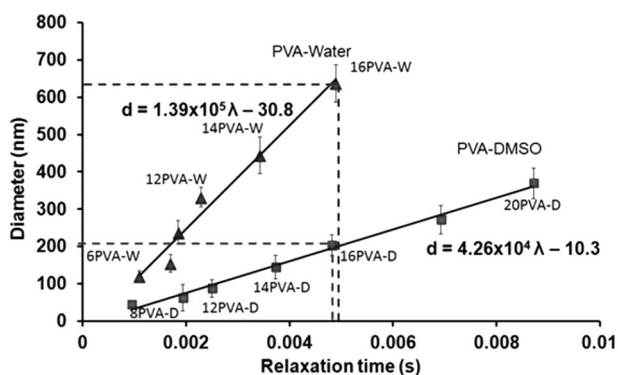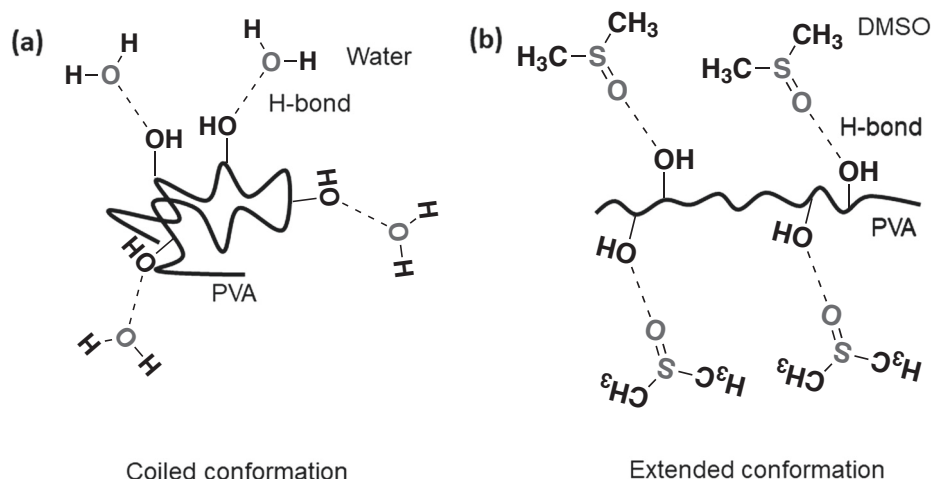

Fig. 9 Plots of diameter vs. relaxation time of PVA–water and PVA–DMSO systems

to the relaxation time. However, the slope of the curve for the PVA-DMSO solutions was lower than that for the PVA-water solutions. Additionally, it was observed that for the same concentration of PVA, the fiber diameters obtained from the PVA-DMSO solution were lower than those obtained from the PVA-water solution, while the relaxation time was similar in both cases (Fig. 9).

This difference in the behavior of PVA in different solvents can again be ascribed to the PVA chain conformations in the two solvents due to polymer-solvent interactions. The fiber diameter for any polymeric system depends upon its ability to form an entangled network. In DMSO, since most of the polymer chains are in an extended conformation (Fig. 10), the tendency to form entanglements is lower. In such systems, the polymer chains interact through the surrounding bulky DMSO molecules, giving rise to a high viscosity but with a lower number of entanglements. This also explains the higher slopes obtained for the semidilute and entangled regions for the plots of specific viscosity versus concentration in PVA-DMSO compared to the PVA-water system (Fig. 2).

During electrospinning, such a solution system (i.e., PVA-DMSO) is expected to offer reduced elastic properties (i.e., resistance to permanent deformation), resulting in higher levels of stretching and thinning, leading to finer fibers. If this hypothesis is valid, then the fiber diameter should have a better correlation with the entanglement density.

Correlation of the fiber diameter of PVA-DMSO and PVA-water with the solution entanglement number $(n_e)_{soln}$

As mentioned earlier, the extended conformation of the PVA chains in DMSO may affect the number of entanglements per chain in the PVA-DMSO system. The number of entanglements in a polymer solution $(n_e)_{soln}$ is given by
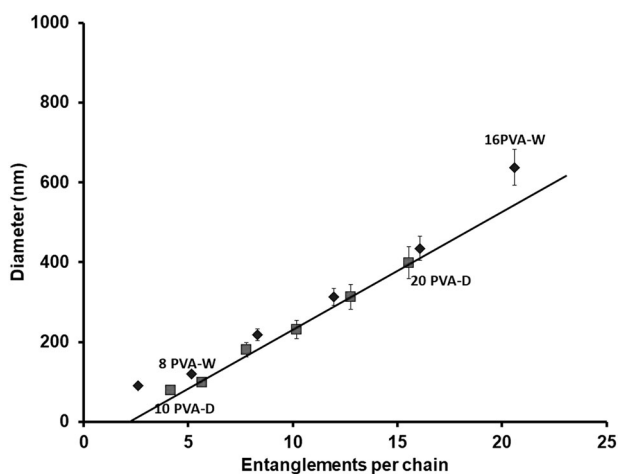

Fig. 10 PVA chain interactions with (a) water and (b) DMSO

Fig. 11 Effects of entanglements per chain on nanofiber diameter for PVA-water (diamonds) and PVA-DMSO (squares) systems

Eq. 4 as described by Shenoy et al. [37].

$$(n_e)_{soln} = \Phi_p(M_w/M_e) \tag{4}$$

where M_w is the molecular weight, Φ_p is the volume fraction of the polymer and M_e is the entanglement molecular weight of PVA, which is reported to be 3750 [41].

Since two different solvents were considered in our study, the volume occupied by the PVA chains in the two solvents (i.e., their volume fractions) can be related to the normalized concentration, i.e., C/C_e, for the two different solvents. Replacing Φ_p by $\Phi_o C/C_e$, Eq. 4 can be rewritten as

$$(n_e)_{soln} = \Phi_o C/C_e x(M_w/M_e) \tag{5}$$

where Φ_o is a constant for a given polymer.

The average entanglement per chain can then be calculated according to Eq. 6.

$$\text{Average entanglement per chain} = (n_e)_{soln} - 1 \tag{6}$$

Plots of the diameter vs. entanglements per chain for both systems are shown in Fig. 11. Interestingly, the diameter could be directly correlated with the average number of entanglements per chain for both solvent systems. As expected, for the same concentration of PVA, the obtained number of entanglements per chain was higher for water than for DMSO. The results suggest that while elasticity may be taken as a controlling factor for determining the diameter in an electrospun fiber, the contribution of elasticity due to entanglements among the chains is of great importance.

Effects of spinning distance and flow rate on the fiber diameters of PVA-DMSO and PVA-water

The effects of spinning distance and flow rate on the fiber diameters of both PVA-DMSO and PVA-water systems
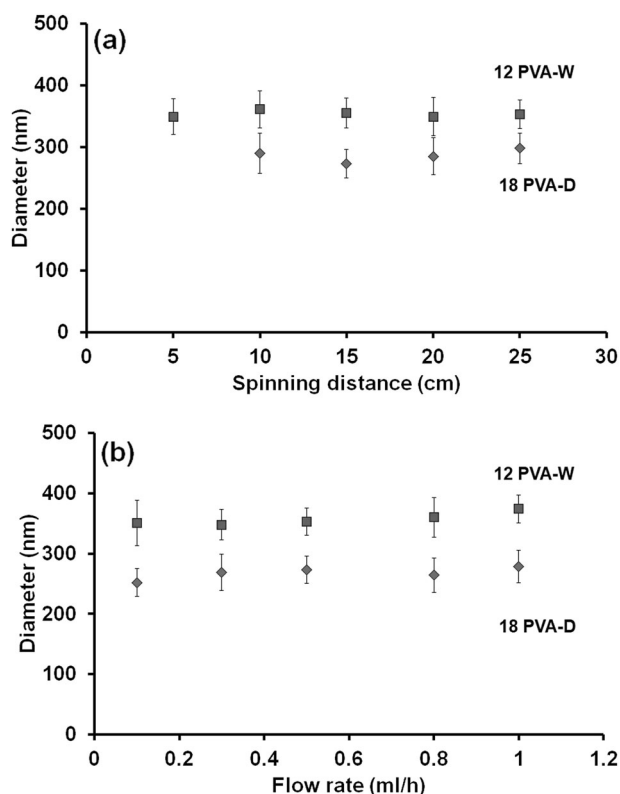

Fig. 12 Plots of diameter vs. (**a**) spinning distance (5–25 cm) at a constant flow rate (0.5 ml/h) and (**b**) flow rate (0.1–1.0 ml/h) at a constant height (25 cm) for 18 wt% PVA-DMSO and 12 wt% PVA-water solutions showing no significant changes in fiber diameter with changing process parameters

were studied. Graphs of the electrospun nanofibers from the PVA-DMSO (18 wt%) and PVA-water (12 wt%) solutions at different spinning distances from 5 to 25 cm and at different flow rates from 0.1 to 1 ml/h are shown in Fig. 12a, b, respectively. SEM images showing the morphology of the electrospun fibers are shown in Fig. 13a, b. The solutions were electrospun under MEV conditions as explained by Basu et al. [32].

No significant change was observed in the fiber diameter either upon increasing the spinning distance or changing the flow rate. For the 12PVA-W solution, an average fiber diameter of 354 ± 10 nm was obtained for all the spinning distances and flow rates studied. Similarly, uniform fibers with an average fiber diameter of 286 ± 13 nm were obtained from the 18PVA-D solution. The data obtained at a spinning distance of 5 cm for 18PVA-D could not be included in the figure as flattening of the fibers was observed (Fig. 12a), indicating incomplete drying of the electrospun fibers at this distance. The statistical analysis showed that there was an insignificant difference in the fiber diameters with a value of $p > 0.05$ for the other electrospun samples.
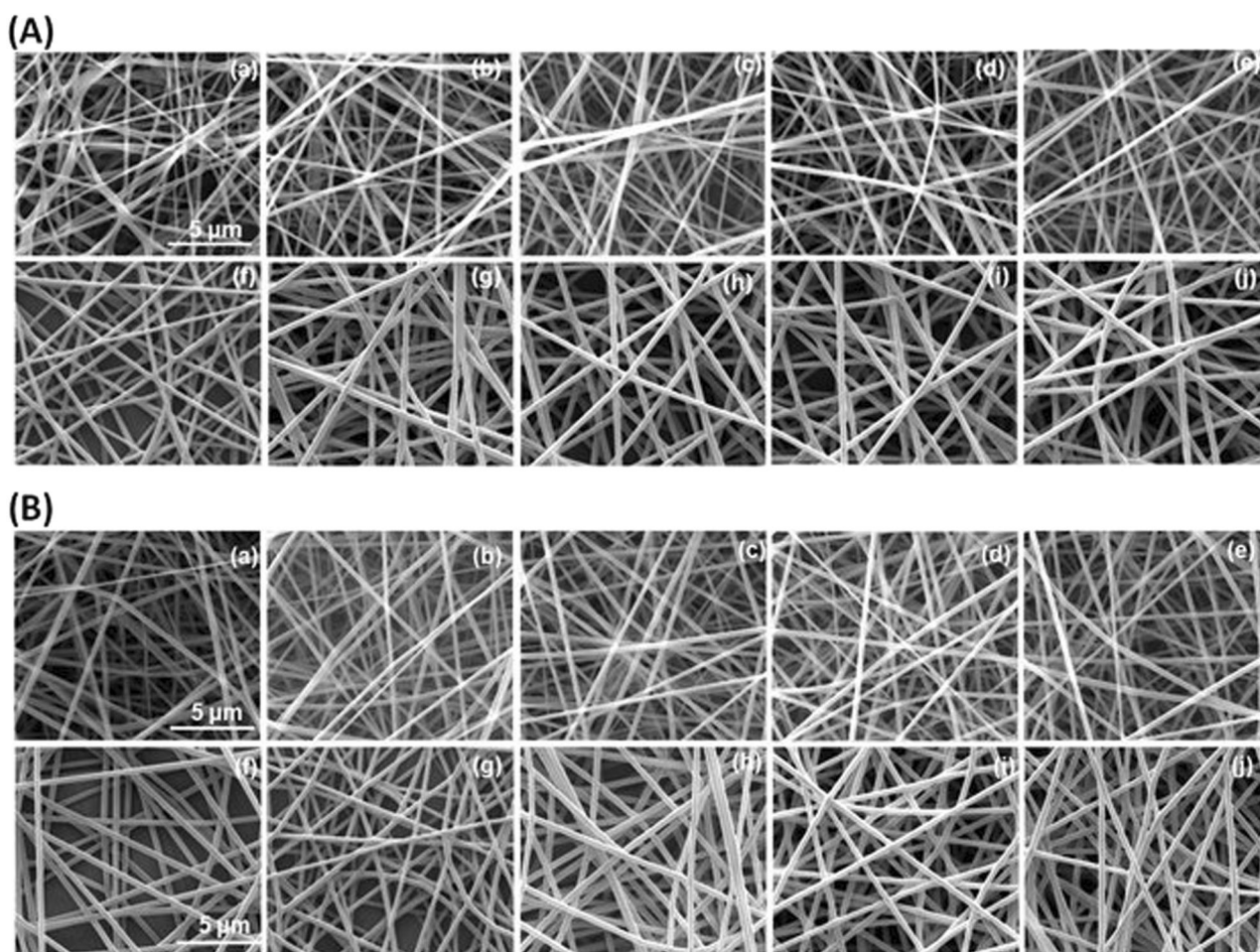
(A)

(B)

Fig. 13 **A** SEM images of nanofibers of PVA from DMSO (**a–e**) and water (**f–j**) for spinning distances of 5 cm (**a** and **f**), 10 cm (**b**, **g**), 15 cm (**c**, **h**), 20 cm (**d**, **i**) and 25 cm (**e**, **j**) at a flow rate of 0.5 ml/h. PVA-DMSO nanofibers show flattening at a distance of 5 cm. **B** SEM images of nanofibers of PVA from DMSO (**a–e**) and water (**f–j**) for flow rates of 0.1 ml/h (**a**, **f**), 0.3 ml/h (**b**, **g**), 0.5 ml/h (**c**, **h**), 0.8 ml/h (**d**, **i**) and 1.0 ml/h (**e**, **j**) at a spinning distance of 25 cm

Comparison of the physical properties of the electrospun nanofibrous membranes

Figure 14a shows comparisons of the tensile stress and tensile strain of the nanofibrous webs obtained from electrospinning of the same amount of polymer from 14PVA-W and 22PVA-D. These solutions were chosen because the fiber diameters obtained by electrospinning were nearly the same (~450 nm) for these samples. The nanofibrous web from PVA-DMSO solution showed a tensile strength of 7.54 MPa and a breaking strain of 33.4%, while that from the PVA-water solution showed a tensile strength of 2.46 MPa and a breaking strain of 41.6%. These results indicate that the nanofibers obtained from the PVA-DMSO solution were much stronger than those obtained from the PVA-water solution. This may be attributed to the fact that PVA molecular chains in DMSO are more extended than those in water, which may result in a better orientation of the chains along the axis of the electrospun fibers.

The thermal transitions of the nanofibers obtained from the PVA-water and PVA-DMSO solutions were investigated using DSC. Figure 14b shows the heat flow curve of PVA-water and PVA-DMSO nanofibers, and the melting peak of the PVA-water nanofibers was at 191.53 °C with an enthalpy of 47.66 J/g. On the other hand, for the PVA-DMSO nanofibers, the melting peak was at a slightly higher value of 193.42 °C with an enthalpy of 56.66 J/g. The percentage crystallinity was calculated from the ratio of the enthalpy of the sample to the enthalpy of 100% crystalline PVA polymer (theoretical value for PVA $Mw \sim 125$ kDa is reported to be 138.60 J/g) [42]. The crystallinity value obtained for the nanofibers from PVA-DMSO was 40.88% and that of PVA-water was lower at 34.38%. The higher melting point and crystallinity obtained in the nanofibers prepared from PVA-DMSO indicate that the oriented polymer chains in the nanofiber may facilitate the formation of a more crystalline phase.
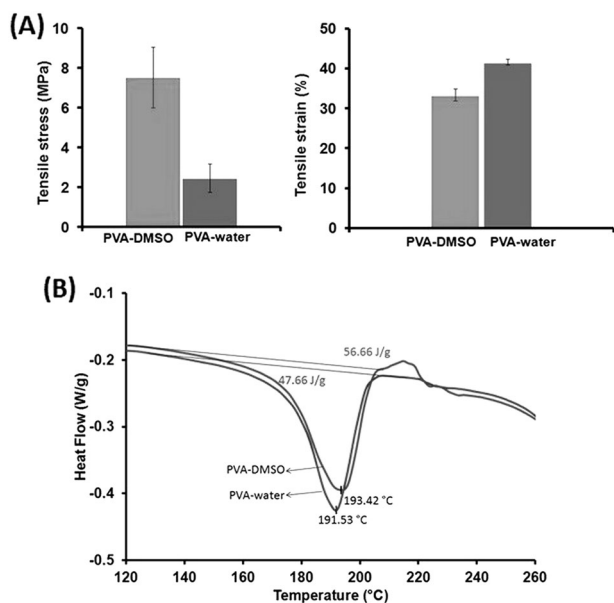
Fig. 14 **A** Tensile strengths and breaking strains of nanofibrous webs from 14PVA-water and 22PVA-DMSO having similar fiber diameters and depositions. **B** DSC thermograms of nanofibers obtained from PVA-DMSO and PVA-water

Conclusions

The rheology and electrospinning behavior of PVA solutions in DMSO and water were investigated to understand the effects of the nature of the solvent. As expected, the viscosity and elasticity of the solutions were found to increase with increasing PVA concentration for both the DMSO and water systems. However, the PVA-DMSO solutions showed significantly higher viscosity and elasticity values than the PVA-water solutions at the same concentrations. Contrary to our expectations, the critical concentration of PVA in DMSO was found to be higher (10 wt %) than that in water (7 wt%). On electrospinning, the fibers obtained from the PVA-DMSO solutions showed much smaller diameters (~63–370 nm for concentrations 10–20 wt %) than those obtained from the PVA-water solutions (120–638 nm for concentrations 6–16 wt%). This atypical behavior was attributed to the polymer chain conformations and the varying degrees of interchain interactions in the two solvents. DMSO, being a better interacting solvent, resulted in extended PVA chain conformations,resulting in pseudoelasticity and hence a lower entanglement density. The direct correlation of the fiber diameter with the entanglements per chain suggested that the elastic component originating from chain entanglements is critical for controlling the fiber diameter. The tensile strength and crystallinity of the nanofiber webs produced from PVA-DMSO were higher by 206 and 18%, respectively, than those obtained from the PVA-water system. The results suggest that the nature of the solvent used in electrospinning can have a significant effect on the morphology and physical properties of the resulting electrospun nanowebs, which may further influence the applicability of the nanowebs.

Compliance with ethical standards

References

1. Kanawung K, Panitchanapan K, Puangmalee S, Utok W, Kreua-ongarjnukool N, Rangkupan R, et al. Preparation and characterization of Polycaprolactone/Diclofenac Sodium and Poly(vinyl alcohol)/Tetracycline Hydrochloride fiber mats and their release of the model drugs. Polym J. 2007;39:369–78.
2. Zeng J, Aigner A, Czubayko F, Kissel T, Wendorff JH, Greiner A. Poly(vinyl alcohol) nanofibres by electrospinning as a protein delivery system and the retardation of enzyme release by additional polymer coatings. Biomacromolecules. 2005;6:1484–8.
3. Zhou Y, Yang D, Chen X, Xu Q, Lu F, Nie J. Electrospun water-soluble carboxyethyl chitosan/poly(vinyl alcohol) nanofibrous membrane as potential wound dressing for skin regeneration. Biomacromolecules. 2008;9:349–54.
4. Kang DH, Kim D, Wang S, Song D, Yoon MH. Water-insoluble, nanocrystalline, and hydrogel fibrillar scaffolds for biomedical applications. Polym J. 2018;50:637–47.
5. Park JC, Ito T, Kim KO, Kim KW, Kim BS, Khil MS, et al. Electrospun poly(vinyl alcohol) nanofibres: effects of degree of hydrolysis and enhanced water stability. Polym J. 2010;42:273–6.
6. Sousa AM, Souza HK, Uknalis J, Liu SC, Gonçalves MP, Liu L. Electrospinning of Agar/PVA aqueous solutions and its relation with rheological properties. Carbohyd Polym. 2015;115:348–55.
7. Supaphol P, Chuangchote S. On the electrospinning of poly(vinyl alcohol) nanofibre mats: a revisit. J Appl Polym Sci. 2008;108:969–78.
8. Koski A, Yim K, Shivkumar S. Effect of molecular weight on fibrous pva produced by electrospinning. Mater Lett. 2004;58:493–7.
9. Li Q, Jia Z, Yang Y, et al. Preparation and properties of poly (vinyl alcohol) nanofibres by electrospinning. In: 2007 IEEE International Conference on Solid Dielectrics, Winchester, UK, 2007, p. 215–8.
10. Rosic R, Pelipenko J, Kristl J, Kocbek P, Bester-Rogac M, Baumgartner S. Physical characteristics of poly (vinyl alcohol) solutions in relation to electrospun nanofibre formation. Eur Polym J. 2013;49:290–8.
11. Papaneophytou CP, Mettou AK, Rinotas V, Douni E, Kontopidis GA. Solvent selection for insoluble ligands, a challenge for biological assay development: a tnf α/spd304 study. ACS Med Chem Lett. 2013;4:137–41.
12. Mano F, Aroso IM, Barreiros S, Borges JP, Reis RL, Duarte ARC, et al. Production of poly(vinyl alcohol) (pva) fibres with encapsulated natural deep eutectic solvent (NADES) using electrospinning. ACS Sustain. Chem Eng. 2015;3:2504–9.

13. Hou Y, Chen C, Liu K, Tu Y, Zhang L, Li Y. Preparation of pva hydrogel with high-transparence and investigations of its transparent mechanism. RSC Adv. 2015;5:24023–30.

14. Kanaya T, Takahashi N, Takeshita H, Ohkura M, Nishida K, Kaji K. Structure and dynamics of poly(vinyl alcohol) gels in mixtures of dimethyl sulfoxide and water. Polym J. 2012;44:83–94.

15. Young TH, Chuang WY. Thermodynamic analysis on the con-onsolvency of poly (vinyl alcohol) in water–dmso mixtures through the ternary interaction parameter. J Memb Sci. 2002;210:349–59.

16. Hoshino H, Okada S, Urakawa H, Kajiwara K. Gelation of poly (vinyl alcohol) in dimethyl sulfoxide/water solvent. Polym Bull. 1996;37:237–44.

17. Hong S, Huang H, Hong P. Effects of solvent adsorption on solution properties of poly (vinyl alcohol)/ dimethylsulfoxide / water ternary systems. Eur Polym J. 2009;45:1158–68.

18. Catalán J, Díaz C, García-Blanco F. Characterization of binary solvent mixtures of DMSO with water and other co-solvents. J Org Chem. 2001;66:5846–52.

19. Zhang P, Zhou T, He L, Zhang S, Sun J, Wang J, et al. Dispersion of multi-walled carbon nanotubes modified by rosemary acid into poly(vinyl alcohol) and preparation of their composite fibres. RSC Adv. 2015;5:55492–8.

20. Uyar T, Besenbacher F. Electrospinning of uniform polystyrene fibres: the effect of solvent conductivity. Polym. 2008;49:5336–43.

21. Tungprapa S, Puangparn T, Weerasombut M, Jangchud I, Fakum P, Semongkhol S, et al. Electrospun cellulose acetate fibres: Effect of solvent system on morphology and fibre diameter. Cellulose. 2007;14:563–75.

22. Sun Z, Deitzel JM, Knopf J, Chen X, Gillespie JW. The effect of solvent dielectric properties on the collection of oriented electrospun fibres. J Appl Polym Sci. 2012;125:2585–94.

23. Eda G, Liu J, Shivkumar S. Solvent effects on jet evolution during electrospinning of semi-dilute polystyrene solutions. Eur Polym J. 2007;43:1154–67.

24. Dreval VE, Malkin AYA, Vinogroaov GV. Effect of the solvent nature on the properties of concentrated solutions of various polymers. Eur Polym J. 1973;9:85–99.

25. Isono Y, Nagasawa M. Solvent effects on rheological properties of polymer solutions. Macromolecules. 1980;13:862–7.

26. Gandhi KS, Williams MC. Effect of solvent character on polymer entanglements. J Polym Sci. 1971;35:2721–5.

27. Kong L, Ziegler GR. Role of molecular entanglements in starch fibre formation by electrospinning. Biomacromolecules. 2012;13:2247–53.

28. Takahashi N, Kanaya T, Nishida K, Kaji K. Effects of con-onsolvency on gelation of poly(vinyl alcohol) in mixed solvents of dimethyl sulfoxide and water. Polymer. 2003;44:4075–8.

29. Gupta D, Jassal M, Agrawal AK. The electrospinning behavior of poly(vinyl alcohol) in dmso–water binary solvent mixtures. RSC Adv. 2016;6:102947–55.

30. Basu S, Gogoi N, Sharma S, Jassal M, Agrawal AK. Role of elasticity in control of diameter of electrospun pan nanofibres. Fibres Polym. 2013;14:950–6.

31. Basu S, Jassal M, Agrawal AK. Concept of minimum electrospinning voltage (MEV) in electrospinning of PAN-DMF system: effect of distance. J Text Insti. 2013;104:158–63.

32. Basu S, Agrawal AK, Jassal M. Concept of minimum electrospinning voltage in electrospinning of polyacrylonitrile N,N-dimethylformamide system. J Appl Polym Sci. 2011;122:856–66.

33. Gupta D, Jassal M, Agrawal AK. Electrospinning of poly(vinyl alcohol)-based boger fluids to understand the role of elasticity on morphology of nanofibres. Ind Eng Chem Res. 2015;54:1547–54.

34. McKee MG, Wilkes GL, Colby RH, Long TE. Correlations of solution rheology with electrospun fibre formation of linear and branched polyesters. Macromolecules. 2004;37:1760–7.

35. Graessley WW. Polymer chain dimensions and the dependence of viscoelastic properties on concentration, molecular weight and solvent power. Polymer. 1980;21:258–62.

36. Colby RH, Fetters LJ, Funk WG, Graessley WW. Effect of concentration and thermodynamic interaction on the viscoelastic properties of polymer solutions. Macromolecules. 1991;24:3873–82.

37. Shenoy SL, Bates WD, Frisch HL, Wnek GE. Role of chain entanglements on fibre formation during electrospinning of polymer solutions: good solvent, non-specific polymer–polymer interaction limit. Polymer. 2005;46:3372–84.

38. Jackson KP, Walters K, Williams RW. A rheometrical study of boger fluid. J Non-Newton Fluid. 1984;14:173–88.

39. Gao H, He J, Yang R, Yang L. Characteristic rheological features of high concentration PVA solutions in water with different degrees of polymerization. J Appl Polym Sci. 2010;116:2734–41.

40. Cho YH, Dan KS, Kim BC. Effects of dissolution temperature on the rheologicalproperties of polyvinyl alchol solutions in dimethyl sulfoxide. Korea-Aust Rheol J. 2008;20:73–7.

41. Tao J, Shivkumar S. Molecular weight dependent structural regimes during the electrospinning of PVA. Mater Lett. 2007;61:2325–8.

42. Peppas NA, Merrill EW. Differential scanning calorimetry of crystalline PVA hydrogels. J Appl Polym Sci. 1976;20:1457–65.